FEATURE ARTICLE

Electrochemical Studies of Enantioselectivity at Chiral Metal Surfaces

Gary A. Attard†

Department of Chemistry, Cardiff University, P.O. Box 912, Cardiff CF10 3TB, U.K.

Received: November 9, 2000

The combination of electrochemical methods with the use of well-defined kinked metal surfaces allows the experimentalist to examine many fundamental aspects of asymmetric reactions at solid surfaces in a new and detailed manner. For example, by systematically changing both the stereogenic center on a particular chemisorbing molecule and also the molecular architecture of the metal surface, relationships between adsorption geometry and reactive sites on the metal surface may be deduced. In addition, by measuring the differential rate of chemisorption of chiral auxiliaries on *R* and *S* metal surfaces insights in to the mechanism of the so-called "Orito" reaction (whereby enantioselective hydrogenation of α-ketoesters is observed) may be deduced. In the present article, a brief resumé of the relevant electrochemical and heterogeneous catalysis literature is expounded together with an analysis of the problem of chirality in two dimensions in order to show that, by utilizing an electrochemical surface science approach, the nature of asymmetric surface reactivity my be tackled in a systematic and accessible manner. Important questions regarding the surface stability or otherwise of chiral modifiers under reaction conditions may be addressed together with the relevance of surface structure in the chemisorption of such species. Some conclusions regarding the mechanism of the Orito reaction on the basis of new experimental data are discussed.

Introduction

In the period of 1979−1980, two remarkable developments were reported[1,2] which have led subsequently to profound changes in our understanding of the reactive interface and, in particular, the role of surface structure and composition in heterogeneous catalysis. The first was the discovery of a heterogeneous catalytic reaction involving the promotion of enantioselectivity in the hydrogenation of prochiral α-ketoesters by the addition of cinchona alkaloids (the so-called "Orito" reaction)[1]:

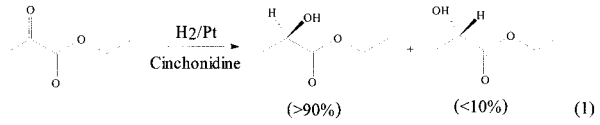

(1)

Although an extensive literature associated with this "simple" reaction has propagated since that time,[3−9] the mechanism by which enantioselectivity is generated within the reaction mixture remains, even after 20 years of research, a subject of some controversy. Today, its resolution is arguably one of the most interesting and certainly most intensively studied areas of research in the whole of heterogeneous catalysis. This is hardly surprising considering the overriding importance attached to asymmetric synthesis and catalysis in all branches of chemistry.[10,11] In electrochemistry, an analogous position is held by the low-temperature electrooxidation of methanol to generate power in fuel cell devices.[12,13] Yet, in both of these catalytic reactions, until fairly recently at least, the structure of the catalyst surface remained somewhat obscured in that only macroscopic measurements (temperature, pressure, bulk composition, potential, current, and capacitance) on polycrystalline materials were available to identify the "active site" and indeed any surface intermediates formed during the reaction.[14−16] The advent of the surface science approach[17] to the study of solid surfaces has contributed enormously to our understanding of many aspects of surface reactivity and emphasized the importance of surface structure and composition in controlling the rates of surface reactions.[18] In this approach, the problem of surface reactivity is reduced to its most basic and simple level. Adsorption studies are performed on clean single-crystal surfaces because such surfaces provide a very limited range of adsorption sites. By introducing, systematically, into the surface defects such as steps, kinks, vacancies, and adatoms, any changes in surface reactivity may be assigned directly to a particular type of adsorption site. The stability of surface intermediates as a function of coverage, surface structure, temperature, and pressure may also be evaluated in a similar manner. Although analogous ex situ surface science measurements are carried out on well-defined electrode surfaces, the method is experimentally demanding and relatively expensive.[19−24] This is because it involves the use of an ultrahigh vacuum (UHV) apparatus, electron spectroscopies which exploit the surface sensitivity of electrons in the kinetic energy range 50−1000 eV,[25] and the bridging between UHV and electrochemical environments.[26] A further criticism, often put, is the question of how relevant measurements on well-defined surfaces under UHV conditions may be to both "real" heterogeneous catalysts operating at

† E-mail: attard@cardiff.ac.uk.

10.1021/jp0041508 CCC: $20.00
Published on Web 03/20/2001

pressures in excess of 1 atm and aqueous electrochemical interfaces. For the electrochemist, the issue of the "pressure gap" between real and model catalytic interfaces is seldom a problem. Nonetheless, similar degrees of surface specificity to those achieved by surface scientists could not be realized in 1979 (with a few notable exceptions as stated previously[19−24]). Despite this, a good deal of structural information concerning the metal−electrolyte interface was known from the use of classical, macroscopic measurements.[27] However, the real breakthrough in the field of *electrochemical surface science* (ESS) came in a seminal paper by Clavilier and co-workers[2] in which it was reported that clean, well-ordered single-crystal surfaces of platinum could be prepared via a simple "flame-annealing" technique. Subsequent work has confirmed Clavilier and co-workers original claims,[2] and over the last 20 years, their paper has spawned a renaissance in studies of well-defined electrode surfaces.[13] The method has been extended subsequently to include other catalytically active metals including gold,[28] rhodium,[29] iridium,[30] and palladium[31] and has enabled electrochemists to perform surface science measurements in situ to a similar, if not higher, degree of precision than analogous measurements in UHV but at a fraction of the cost. In situ scanning probe microscopies attest to the high quality of the surfaces prepared via the flame-annealing technique.[28−32] As a consequence, new electrochemical phenomena are regularly being reported which are attributable solely to the extent of atomic and molecular long-range surface order.[24] The structural sensitivity of electrocatalytic reactions has also been made manifest in such studies.[13,33−38]

The aim of the present article is to illustrate how the ESS approach was used to demonstrate, for the first time, the intrinsic chirality of certain types of clean metal single-crystal surfaces and how the method may be applied directly to problems of enantioselectivity in heterogeneous catalysis. Because of the presence of two condensed phases, the electrode surface is never "clean" in the sense surface scientists refer to well-defined surfaces. In fact, electrochemical processes of adsorption and desorption should always be thought of as replacement reactions of one surface active species by another as a function of potential and electrolyte composition. Nonetheless, important insights into the nature of catalytic activity may be obtained because the electrochemical technique of choice, cyclic voltammetry (CV),[39] is particularly sensitive to changes in the *local charged state of different surface regions* (terraces, steps, kinks, adatoms, and chemisorbates),[40,41] and hence, perturbation of these surface sites as a consequence of chemical reaction may readily be identified. An analogous surface science tool would be photoemission from adsorbed xenon (PAX) which not only locks into the local work function of a surface site but also provides quantitative estimates of local surface coverages.[41,42] Finally, the present status of the Orito reaction will also be discussed and a partial assessment made of the reaction mechanism on the basis of some new electrochemical findings from our laboratory. A number of key questions will be addressed:

(i) What criteria need to be satisfied in order that a clean metal surface may become chiral?

(ii) How may one prepare such chiral metal surfaces?

(iii) What influence could surface chirality have on the Orito reaction and other enantioselective heterogeneous reactions?

(iv) Can ESS methods be used to elucidate the mechanism of the Orito reaction?

The answers to questions iii and iv are still very much the subject of intensive experimental investigation. It is hoped nonetheless that some of the excitement of this still very young field of physical chemistry research may be experienced by the reader who may in turn wish to contribute their own expertise to bring about a clearer understanding of asymmetric reactions in two dimensions.

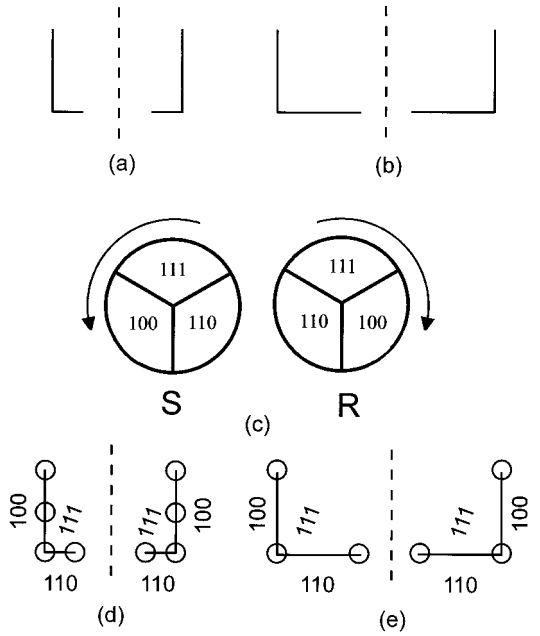

Figure 1. Schematic representations of metal kink sites illustrating the nature of the surface chirality according to refs 44 (a and b) and 51 and 52 (c−e; see text for details).

Chirality at Clean Metal Surfaces

Low Miller index planes of ceramic crystals containing an asymmetric bulk unit cell are naturally chiral.[43] However, the surfaces of face centered cubic (fcc) metals are not normally thought of in the same way. It was Gellman et al[44] who pointed out that sites associated with certain kinked single-crystal metal surfaces may be considered as being chiral so long as the two steps constituting the kink site were of unequal length.[44] For example, if one tries to place Figure 1a onto its mirror image without leaving the plane of the paper, it is found that the images are nonsuperimposable, i.e., the kink site is chiral. In contrast, when Figure 1b is rotated by 90° in the plane of the page, it is completely superimposable on its mirror image, i.e., because the magnitudes of the step lengths on either side of the kink are the same: the kink is achiral.

To test this hypothesis concerning the intrinsic chirality of metal kink sites, one first requires a chiral probe. Gellman and co-workers[44] chose to investigate the adsorption and desorption of the simplest chiral alcohol, 2-butanol, on an appropriate chiral kinked surface, namely, Ag{643} and its enantiomorph Ag{$\overline{643}$}. The {643} plane may be written in microfacet notation[45] as 3{111} × {310}, i.e., a three atom wide {111} terrace separated by zigzag {310} steps. Within the precision of their experimental technique (thermal desorption),[25] no enantioselectivity could be detected in the desorption of (*R*)- or (*S*)-2-butanol on either of the chiral kinked silver surfaces. Despite this, these workers were the first to examine the chirality of metal surfaces in such a systematic and detailed manner. Very soon after this work was published, theoretical calculations by David Sholl pointed to the fact that many adsorption systems were *expected* to show detectable enantiospecific energy differences.[46] Having read the Gellman and Sholl papers, we decided to look again at the enantioselectivity of kinked metal surfaces from an electrochemical perspective, but instead of

using a simple molecule containing just one chiral center (2-butanol) as chemisorbate, D-glucose was chosen because it contained (at least) five chiral centers. From an electrochemical standpoint, D-glucose is not the chiral probe of choice because of the complexity of its electrooxidation reaction in aqueous solutions.[47−49] However, it can be obtained in very pure form, and its enantiomer, although expensive, is commercially available. Also, a somewhat more reactive electrode surface was thought necessary to activate the organic molecule, and so the enantiomeric pairing of Pt{643} and Pt{$\bar{6}43$} was chosen instead of the corresponding silver surfaces. In addition, we realized that the "Gellman" interpretation of chirality in metal surfaces, although essentially correct, could only be an approximation because it failed to take into account the microstructure of individual steps comprising the kink site. This point is illustrated in Figure 1c, whereby a kink site may be thought of as the junction of three fundamental sites, namely, {111}, {100}, and {110}. Each of these may correspond to a terrace, with the other two becoming the step sites forming the kink. Using a Cahn−Ingold−Prelog analysis[50] with a substituent priority in terms of atomic surface density, the hierarchy of surface sites becomes {111} > {100} > {110} for fcc metals. Hence, an *R*-chiral kink may be identified if the sequence {111} → {100} → {110} viewed from the vacuum or electrolyte side runs clockwise and an *S*-chiral kink if the sequence runs anticlockwise. In Figure 1 parts d and e, the individual character of the step and terrace sites is now included into the schematic of Figure 1 parts a and b. Although the kink in Figure 1d is still chiral by virtue of its inequality in step lengths, it is also chiral because of the nonsuperimposability of the kink microstructure. Of particular note, however, is that now Figure 1e displays chiral properties despite the equivalence of the magnitudes of the step lengths forming the kink. Hence, in our analysis, *all* kinked single-crystal metal surfaces are chiral so long as the kink site incorporates three different types of fundamental sites. A more detailed exposition of the surface crystallography of kinked surfaces may be found in ref 51.

Verification of the Intrinsic Chirality of Kinked Single-Crystal Metal Surfaces

Experimentally, the preparation of chiral platinum surfaces is rather straightforward. To prepare a Clavilier bead single crystal,[2] the electrode is first oriented (using either a He−Ne laser[51] or Laue backscattering) as shown in Figure 2, whereby the various crystallographic directions are represented by a family of eight stereographic triangles. The stereographic triangles alternate as *R* or *S* as may be deduced by taking the sequence of sites {111} → {100} → {110} for each triangle.

Kinked surface planes correspond to all points located within a stereographic triangle, and hence, all points lying on the sides or at the vertexes of the stereographic triangle are associated with achiral surfaces. Rotation angles in the plane defined by moving from the (100) to the (111) pole we define as α, and rotations orthogonal to this plane (rotations from the (111) to the (110) pole for example) we define as β. It is evident that in order to produce an *R* surface starting at the (100) pole, two angles of rotation are required, α followed by $N\beta$ (see Figure 2). However, to orientate the crystal to produce the corresponding *S* surface, a rotation of α followed by $N\beta$ is needed. Once the bead electrodes are oriented, the *R* and *S* planes may be produced by grinding and polishing.[51] Flame-annealing and cooling in hydrogen (care!) of the polished crystal will subsequently give rise to a clean, well-ordered (1 × 1) surface as judged by LEED and AES,[52] at least for surfaces based on kinked {111} terraces.

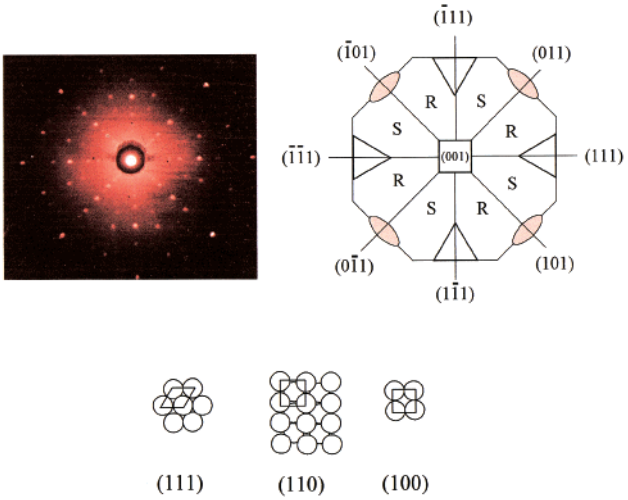

Figure 2. Laue backscattering photograph from a Pt{001} oriented crystal together with a simplified stereographic projection to illustrate the nature of surface chirality. The fundamental adsorption sites for fcc crystals are also shown. *R* stereographic triangles corresponds to the sequence (111) → (100) → (110) being clockwise and *S* stereographic triangle to the anticlockwise arrangement.

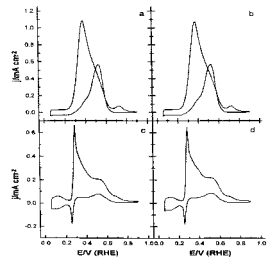

Figure 3. (a) and (c) CVs of D-glucose electrooxidation on achiral Pt{111} and Pt{211} respectively. (b) and (d) CVs of L-glucose electrooxidation on achiral Pt{111} and Pt{211} respectively. 0.1 M H_2SO_4 + 5 × 10^{-3} M glucose. Sweep rate = 50 mV/s.

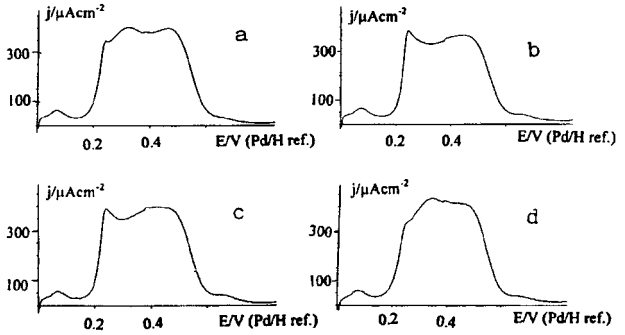

Figure 4. (a) and (b) CVs of D-glucose electrooxidation on Pt{643}^{S} and Pt{643}^{R}, respectively. (c) and (d) CVs of L-glucose electrooxidation on Pt{643}^{S} and Pt{643}^{R}, respectively. 0.1 M H_2SO_4 + 5 × 10^{-3} M glucose. Sweep rate = 50 mV/s.

Figure 3 shows the CVs of the initial glucose electrooxidation currents on Pt{111} and Pt{211}. As expected, no difference in the voltammetric profile is discerned between D- and L-glucose for both of these electrodes because they are achiral (the Pt{211} surface consists of three atom wide {111} terraces, like Pt{643}, but the terraces are separated by *linear* {100} × {111} steps). The major oxidation currents at 0.38V/RHE (Pt{111}) and 0.29V/RHE (Pt{211}) correspond to the maximum rate of glucose decomposition on {111} terraces and {100} × {111} steps respectively.[47] In contrast, when Pt{643} is used, a clear enantiomeric response is obtained (Figure 4). In terms of voltammetric profile:

$$\text{Pt}\{643\}^S + \text{D-glucose} \equiv \text{Pt}\{643\}^R + \text{L-glucose}$$

and

$$\text{Pt}\{643\}^S + \text{L-glucose} \equiv \text{Pt}\{643\}^R + \text{D-glucose}$$

Hence, a classical diastereomeric result involving two stereogenic centers is realized, and as such, this measurement constitutes the first experimental confirmation of the intrinsic chirality of kinked metal single crystals. A more detailed inspection of Figure 4 reveals that, for the Pt{643}^{S}/D-glucose and Pt{643}^{R}/L-glucose pairing, the peak at 0.33V/Pd−H (reaction at {111} terraces) is larger than the 0.22V/Pd−H peak (reaction at {111} × {100} steps), whereas the reverse is true for the alternate pairing of chiral surface and glucose. Interestingly, negligible glucose decomposition (as measured by the magnitude of the electric current density at 0.07V/Pd−H) takes place at the {110} step site of the kink. This finding has been replicated for a number of sugars including mannose, arabinose, and xylose[53,54] and for other kinked surfaces including Pt{531}, Pt{321}, and Pt{431}. Clearly the {110} site must play a role in initially orienting the carbohydrate molecule in relation to the handedness of the kink, but the actual bond-breaking, surface reactions appear to proceed most readily at the {100} and {111} sites. The structural sensitivity of the glucose electrooxidation reaction may also be seen when the surface density of kink sites is varied. This is exemplified in Figure 5, whereby increasing the surface density of kinks on going from Pt{643} to Pt{321} to Pt{531} leads to a greater and greater degree of electrochemical enantioselectivity for the electrooxidation of glucose. By electrochemical enantioselectivity, it is meant the ratio of the difference in electrooxidation current (reaction rates) over their sum for a given *R* and *S* surface at a fixed potential υ.

$$S = \frac{I_R(\upsilon) - I_S(\upsilon)}{I_R(\upsilon) - I_S(\upsilon)} \times 100\%$$

For reaction at {111} terrace sites (0.38V/Pd−H)

$$S\,(\text{Pt}\{643\}) < S\,(\text{Pt}\{321\}) < S\,(\text{Pt}\{531\})$$

Interestingly, the *absolute* magnitude of all electric currents decreased on going from the less kinked to the most kinked surface. This is in accordance with expectations of the structure sensitivity of glucose electrooxidation in that the rate is found to increase markedly with increasing terrace width.[48,49] Nonetheless, it appears that for glucose electrooxidation, at least, *S* scales with the surface density of kinks. Also, by measuring *S* as a function of temperature, for Pt{643}, a difference in activation energy for glucose electrooxidation on *R* and *S* surfaces of $\cong$ 1−2 kJ mol^{-1} has been estimated[52] in good agreement with theoretical calculations.[46] However, as stressed in ref 55, not every pair of chiral molecule and chiral surface will exhibit sizable enantiospecificity in adsorption related properties. In fact, the degree of enantiospecificity should depend critically on the property of interest. For example, as mentioned earlier, the difference in desorption enthalpy of 2-butanol on *R* and *S* Ag{643} is beyond the detection limit of TPD. However, recent measurements using FTIR indicate that chemisorbed methylcyclohexanone adopts two distinct chiral geometries.[56] In fact, in accordance with a recent theoretical paper, processes such as surface relaxation can sometimes exert an even greater influence than kink surface density, surface structure, or molecular configuration on the chiral discrimination mechanism.[56]

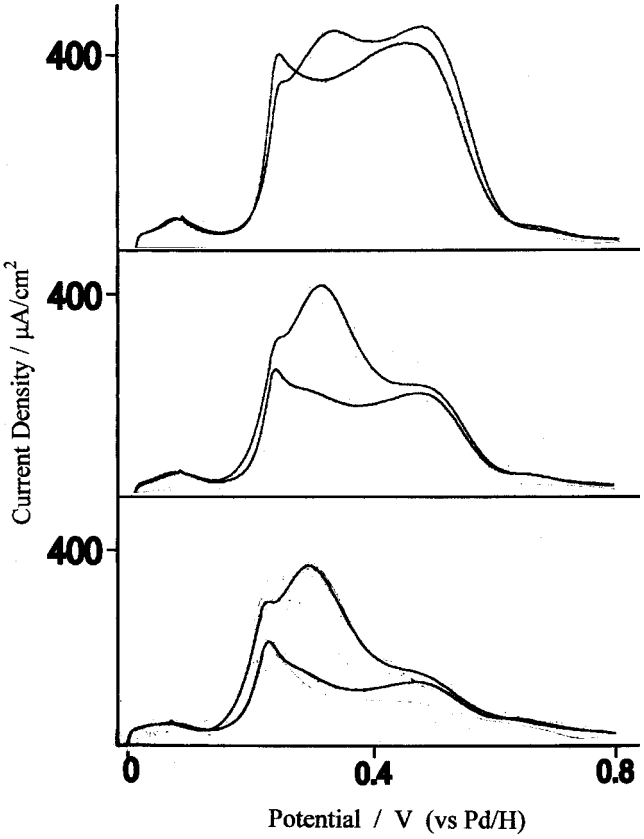

Figure 5. CVs of Pt{643}^{S} and Pt{643}^{R} (top), Pt{321}^{S} and Pt{321}^{R} (middle), and Pt{531}^{S} and Pt{531}^{R} (bottom) in 0.1 M H_2SO_4 + 5 × 10^{-3} M glucose. Sweep rate = 50 mV/s. As surface kink density increases, so too does electrochemical enantioselective excess *S* (see text).

Figure 6 shows the CVs of glucose electrooxidation using Pt{431}^{R} and Pt{431}^{S} electrodes. Pt{431} is related to Pt{643} in that its {111} terrace width is ostensibly the same (although only at its greatest extent), but the magnitudes of the {110} and {100} step lengths are interchanged, i.e., whereas the kink sites of Pt{643} possess a long (3 atom) {100} step and a short {110} (monatomic) step, Pt{431} possesses long (3 atom) {110} steps and short (monatomic) {100} steps. Through a modification of the "molecular architecture" in this way, it is possible to change the potential of greatest *S* from 0.42 V/RHE ({111} terraces) on Pt{643} to 0.27 V/RHE ({100} steps) on Pt{431}. Note again that negligible electrooxidation currents are generated at the {110} sites (0.05 V/RHE). Hence, it is possible, by varying the molecular architecture of the kinked surface, to tailor the electrocatalytic properties of the electrode in a rather systematic manner. However, it is more usual in organic chemistry to change the stereocenter on the organic molecule and then measure changes in reactivity and chiral discrimination in order to elucidate reaction mechanisms. In the next section, this approach will be applied for the first time, to identify the reactive center on the chemisorbate molecule undergoing enantioselective electrooxidation.

Enantioselective Electrooxidation—Identification of the Reactive Sites via Systematic Variation in Stereogenic Center

In essence, a two-dimensional analogue of an isotopic substitution experiment is being attempted, but instead of changing the mass of a carbon atom, a change in the "handedness" of a single carbon center is utilized.[53] A series of related

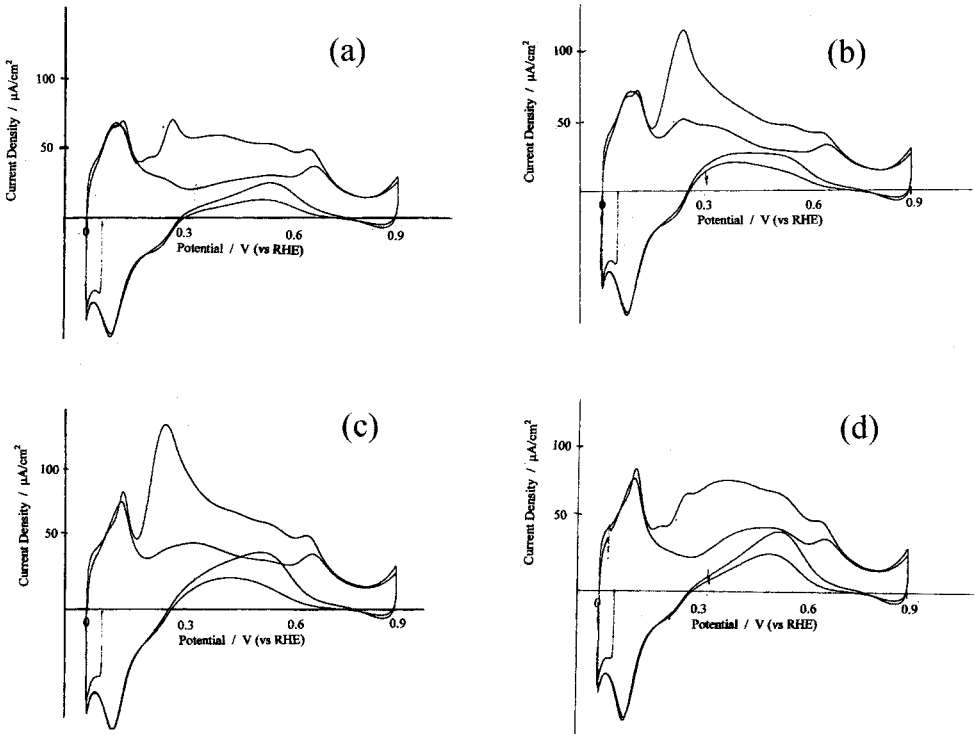

Figure 6. (a) and (b) CVs of L- and D-glucose electrooxidation respectively on Pt{431}^{R}. (c) and (d) CVs of L- and D-glucose electrooxidation respectively on Pt{431}^{S}. 0.05 M H_2SO_4 + 5 × 10^{-3} M glucose. Sweep rate = 50 mV/s. From ref 54.

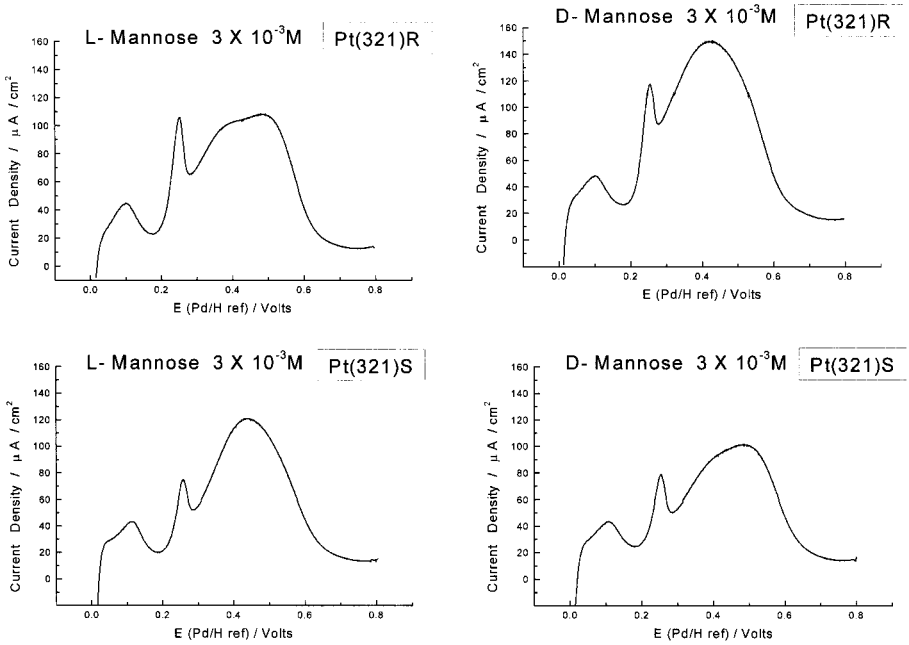

Figure 7. CVs showing diastereomeric results of electrooxidation of D- and L-mannose on Pt{321}^{R} and Pt{321}^{S}. Peak A is situated between 0.3 and 0.4V. 0.1 M H_2SO_4 + 3 × 10^{-3} M mannose. Sweep rate = 50 mV/s. From ref 53.

sugars—glucose, mannose xylose, and arabinose—are allowed to adsorb onto a chiral kinked platinum electrode, and the initial electrooxidation current is monitored. Although each sugar gives rise to its own singular response, a number of features are common to all CVs. The most important being the absence or presence of a peak at (0.35−0.4V (Pd/H)) corresponding to reaction at {111} terraces (we shall from now on refer to this feature as peak A). For D-glucose/*R* kinks and L-glucose/*S* kinks, peak A is not present whereas for D-glucose/*S* kinks and L-glucose/*R* kinks it may clearly be discerned (see Figure 4). Figure 7 shows the diastereomeric result of reacting mannose with the same *R* and *S* electrodes. Note that, although the CVs differ from those of glucose, once again the presence of peak A is indicated for the D/*S* and L/*R* combination, whereas it is not present for the D/*R* and L/*S* pairing. Glucose and mannose are epimers differing only in the chirality of the carbon atom at position 2. This suggests that changing the stereogenic center at this position does not in itself alter the chiral relationship between the chemisorbate and the metal surface. In contrast, when D- and L-arabinose were investigated, it was found that peak A was present for the D/*R* combination but not present for the D/*S* (Figure 8). There are two differences between arabinose and glucose. The first is the change in chirality at carbon atom position 3. The second is that arabinose does not contain a

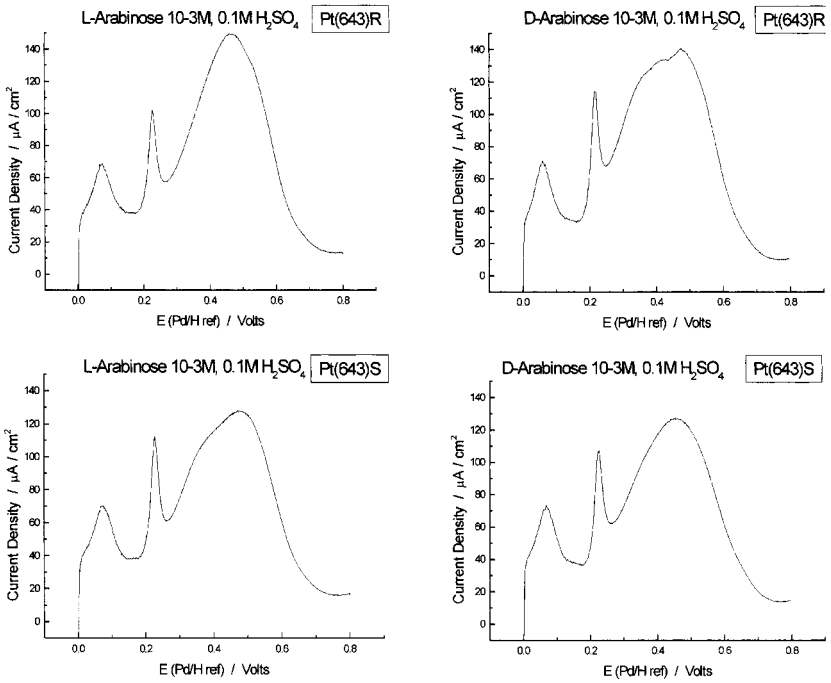

Figure 8. CVs showing diastereomeric results of electrooxidation of D- and L-arabinose on Pt{643}^{R} and Pt{643}^{S}. Note that, in contrast to Figure 7, peak A is now only absent with the D + *R* and L + *S* combinations. 0.1 M H_2SO_4 + 1 × 10^{-3} M arabinose. Sweep rate = 50 mV/s. From ref 53.

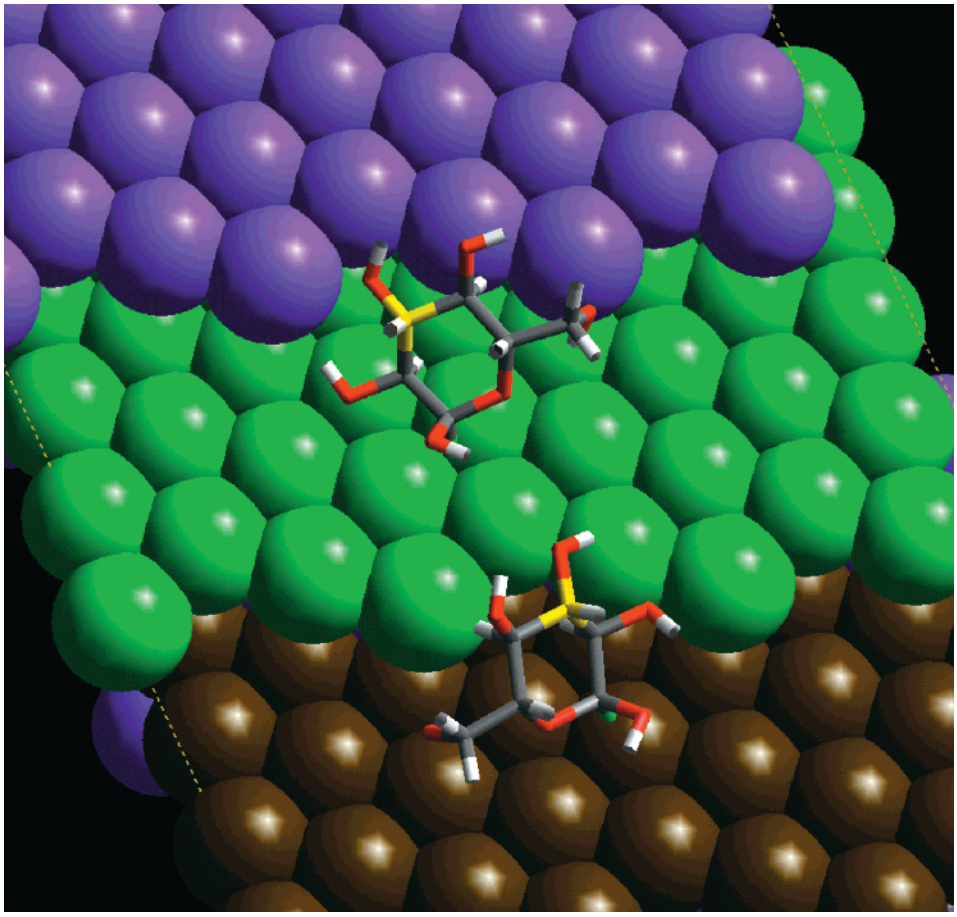

Figure 9. Schematic showing interaction of chiral carbon center 3 (highlighted in yellow) with a chiral Pt{643}^{S} surface for D- (top) and L-glucose (bottom). To be consistent with previous data from ref 48, the hydrogen at position 1 is directed toward the (111) terrace and has been colored green.

CH_2OH substituent at ring position 5. Either of these two features could mark out arabinose from glucose. However when xylose is investigated (which like arabinose does not contain a CH_2OH group at position 5), the *S*/D and L/*R* combinations do give rise to peak A, just like glucose and mannose. Because xylose possesses the same chirality as glucose and mannose at

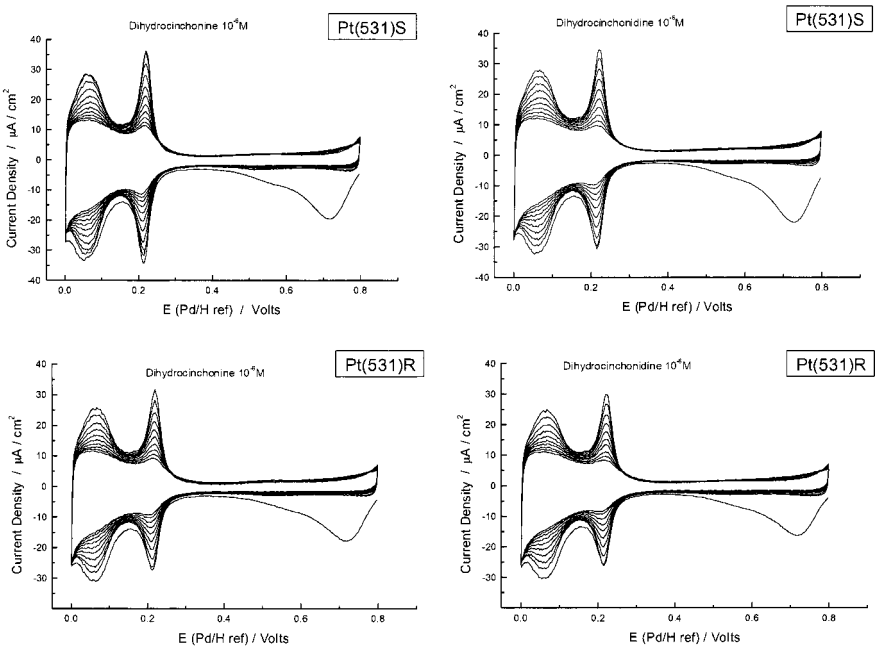

Figure 10. Dihydrocinchonidine and dihydrocinchonine uptake on Pt{531}^{R} and Pt{531}^{S}. 0.1 M H_2SO_4 + 10^{-6} M alkaloid. Sweep rate = 50 mV/s.

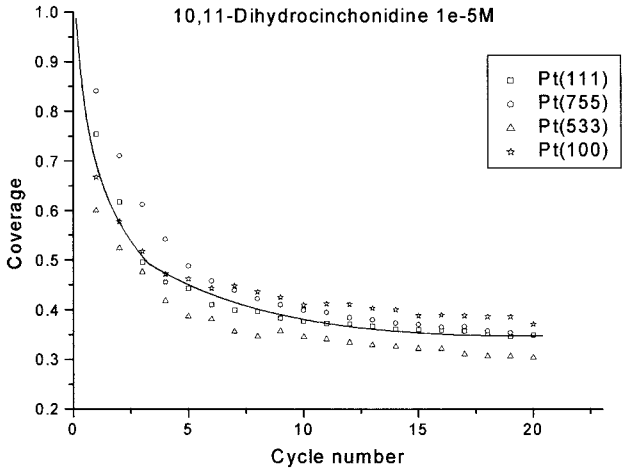

Figure 11. Variation in coverage of free metal sites as a function of the number of potential cycles (time) for achiral platinum electrodes. 0.1 M H_2SO_4 + 10^{-5} M dihydrocinchonine. Sweep rate = 50 mV/s, and the upper and lower potential limits were 0 V and 0.8 V (Pd/H), respectively. The black line is meant as a guide to the eye.

position 3, whereas in arabinose the chirality is reversed, we suggest that chiral discrimination between the glucose at carbon 3 and the kink gives rise to the enantioselective reaction associated with peak A. It is well-known that sugars undergo mutarotation in aqueous solution to produce the α and β forms of pyranose and furanose. However, for all of the sugars studied, the percentage of furanose in solution should be negligible.[57] For the pyranoses in aqueous solution, mannose and arabinose give rise to 60% and 40%, whereas for xylose and glucose, the proportions are 64% and 36%. Hence, speciation behavior *cannot* account for the enantioselectivity displayed by the four sugars in relation to peak A. Combining this information with the seeming lack of reactivity of the {110} site and the knowledge from previous isotopic substitution experiments on glucose that initial C−H bond cleavage at carbon position 1 takes place on Pt{111},[48] together with the variation in *S* upon changing kink density and shape, it may be possible to begin modeling the interaction of chiral molecules with chiral kinks in a new and fundamental manner. Results from such modeling calculations will be presented in a future publication. In Figure 9, an optimized structure for the D- and L-glucose on Pt{643}^{S} is shown. The chiral center at position 3 has been positioned as close to the chiral kink site as possible. In addition, the hydrogen−carbon bond at position one, which is known to dissociate during the glucose electrooxidation reaction,[48] has been directed toward the (111) terrace.

Electrochemical Investigations of the Enantioselective Hydrogenation of α-Ketoesters—The Role of the Chiral Auxiliary

In reaction 1, the function of the chiral auxiliary in steering the enantiospecificity of the reaction is of prime importance. Two key (and competing) theories of the *modus operandi* of the cinchona alkaloid have been postulated:

(i) formation of a modifier−substrate complex between methyl pyruvate and cinchonidine at the platinum surface leading to hydrogenation of the prochiral carbonyl group to give a single stereochemical configuration of the final product[7−9]

(ii) complexation of the α-ketoester with the cinchona alkaloid *in solution* giving rise to a "shielding effect" on one side of the prochiral carbonyl group of the α-ketoester. Subsequent hydrogenation of this solution complex either via an Eley−Rideal mechanism or via surface decomposition and addition of hydrogen (Langmuir−Hinshelwood) gives rise, subsequently, to the enantioselectivity observed.[7−9,57−60]

Certainly the Eley−Rideal mechanism may be excluded on the basis of kinetic measurements.[8] However, both of the remaining models are consistent with the reaction kinetics.[8] Interestingly, recent detailed surface science studies have demonstrated that well-ordered arrays of the chiral modifier tartaric acid can form on copper surfaces which in turn create "chiral runways",[61] free metal sites of a single type of handedness, capable of providing the necessary surface complexation site to generate an enantiospecific interaction with the prochiral keto group (model i). For platinum surfaces, however, only disordered alkaloid overlayers have ever been reported.[62] In addition, the assumption of a "half-hydrogenated" intermediate

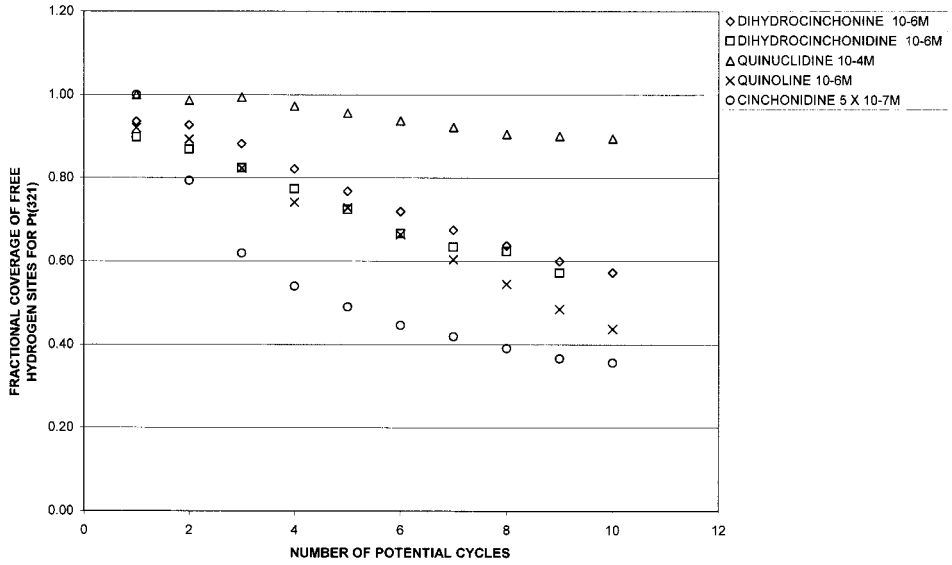

Figure 12. Plot of fractional coverage of free hydrogen sites vs number of potential cycles (time axis) for uptake of various organic molecules from 0.1 M H_2SO_4 on Pt{321}^{R}. See inset key for concentration and nature of organic adsorbate.

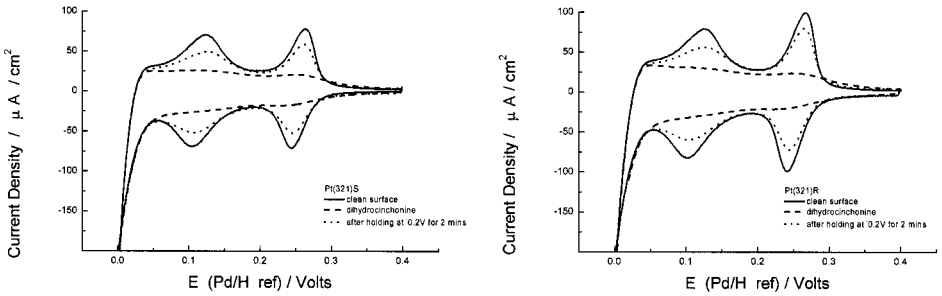

Figure 13. Hydrogen-induced desorption of dihydrocinchonine from Pt{321}^{S} and Pt{321}^{R}. Clean surface of hydrogen electrosorption region (—); after adsorbing saturated layer of dihydrocinchonine (- - -); after holding the dihydrocinchonine adlayer at −0.2 V (Pd/H) for two minutes showing recovery of free platinum sites (•••). Note that bubbling H_2 at 1 atm pressure while holding the electrode potential at 0 V gave rise to a similar result.

adsorbed parallel to the metal surface (an important assumption of model i) has been challenged by recent FTIR and photoemission studies of methyl pyruvate adsorption on clean Ni-{111}[63] and Pt {111}[64] in UHV, showing that this chemisorbate almost certainly prefers an upright, vertical coordination, bonding via the lone pairs on the oxygen atoms to the metal surface, hence, leading logically to racemic hydrogenated products.

It should be recognized that the "shielding" model is already well-understood and accepted as viable in many asymmetric homogeneous organic reactions,[65] although the sensitivity of the heterogeneous reaction to many structural and compositional aspects of the catalyst surface would remain unanswered by this model.[7−9] However, it is evident that all existing models of the enantioselectivity of reaction 1 *ignore the intrinsic chirality of the metal catalyst*, i.e., in reality such particles should more correctly be referred to as *racemates* containing equal numbers of *R* and *S* kinks. If the proportions of *R* and *S* kinks could be altered by preferential adsorption of one or more components of the reaction mixture, it would also provide a satisfactory model of the enantioselectivity of reaction 1 without the need for extended (ordered) arrays of chiral modifiers and including explicitly, the sensitivity of the reaction to catalyst morphology and preparation methods. The question remains nonetheless as to what species could be adsorbed preferentially Two possibilities may be considered:

(a) that cincona alkaloids, like the pyranoses alluded to earlier, exhibit a chiral response when adsorbing on *R* or *S* kinks

(b) that a modifier/α-ketoester complex exhibits the necessary chiral discrimination between *R* and *S* kinks.

Model a may be addressed directly by following the adsorption of 10,11-dihydrocinchonidine and 10,11-dihydrocinchonine (the "near enantiomer" of dihydrocinchonidine) on *R* and *S* single-crystal electrodes from aqueous acidic solutions (Figure 10). The uptake of alkaloid is signified by the attenuation of peaks at 0.07 V ({110} sites), 0.22 V ({100} sites), and 0.5 V ({111} terraces). Strictly, these {111} sites should not be observed on Pt{531}, but a slight mis-cut of the crystals has led to a very small voltammetric intensity associated with their presence. More importantly, however, unlike for the case of the pyranoses, no chiral discrimination is observed, i.e., the attenuation in all clean surface peaks, irrespective of the alkaloid/chiral surface combination, occurs at the same rate. This has also been observed using Pt{643}.[53] When such adsorption rate studies are extended to flat and stepped achiral surfaces, again little change in the rate of alkaloid adsorption obtains (Figure 11).[66] This "indiscriminate" adsorption by the alkaloid suggests that structural models from the literature based on particular terrace widths and particle sizes do not seem to play a central role in determining the mechanism of enantioselectivity at least so far as the alkaloid in the absence of other reactants is concerned. Rather, all sites (step, terrace, and kink) appear to be occupied with equal probability during adsorption from solution consistent with a random distribution of alkaloid chemisorbate. This is also in agreement with previous LEED results.[62] It was noted during these electrochemical adsorption

measurements that it was impossible to block *all* of the platinum sites by the alkaloid, with perhaps 30−40% of platinum sites remaining free of adsorbate (see Figure 11).[66] Again this supports a random distribution of alkaloid molecules exhibiting limited surface mobility and leading to "gaps" in the overlayer, insufficiently large to accommodate further uptake of alkaloid molecules.

By consideration of the quinoline and quinuclidine groups which make up the cinchona alkaloid, it is also possible to address electrochemically the configuration of the molecule adsorbed on the surface. Figure 12 shows a graph of normalized voltammetric peak area (1 = clean surface, 0 = complete blocking) vs the number of potential sweeps (essentially a time axis). It is clear that when the alkaloid and quinoline are considered (at 10^{-6} M concentration), the initial rates of adsorption (gradient) match closely. There is some divergence at higher coverages, perhaps associated with the difficulty of packing cinchona alkaloids relative to quinoline rings. For quinuclidine, even for ×100 more concentrated solutions, a relatively low rate of adsorption is found. From these measurements, one may conclude that alkaloid adsorption must be occurring via the quinoline ring and that the quinuclidine substituent does not interact very strongly with the metal surface. These findings are in agreement with previous H/D exchange data[67] and recent NEXAFS studies showing that the quinoline ring of the alkaloid adsorbs parallel to the metal surface at room temperature.[68]

Although the results outlined above appear to negate the possibility of preferential adsorption of the alkaloid at kink sites, it must be remembered that there is good evidence that under reaction conditions, a dynamic equilibrium is achieved with competition for surface sites by dihydrogen, alkaloid, solvent, and α-ketoesters.[8] To assess the stability of the chemisorbed alkaloid under reaction conditions, CV was used to monitor the surface coverage of alkaloid after exposure of the surface to 1 atm of hydrogen for a few minutes. It is evident from Figure 13 that the adlayer is unstable in the presence of hydrogen gas, as demonstrated by the almost complete recovery of platinum adsorption sites. Furthermore, reductive *desorption* of alkaloid from the surface appears also to be a racemic reaction with no evidence of preferential desorption from particular *R* or *S* kinks.[53] Hence, the actual concentration of alkaloid on the surface under reaction conditions (50 atm hydrogen pressure) is probably small. Another noteworthy feature stemming from the measurement of the rate of irreversible adsorption of modifiers was that chemisorbed oxygen adatoms inhibit the uptake of alkaloid.[53] Whether the surface concentration of oxygen adatoms ever reaches the surface coverages typical of those of a freshly flame-annealed Pt crystal (0.25 monolayers) in the presence of 50 atm of hydrogen is debatable, but it is interesting that reaction 1 is reported to give rise to poor enantioselective excess under strictly anaerobic conditions.[69] Hence, ironically, the presence of hydrogen and oxygen in the reaction mixture, at least according to our results, should act to keep the alkaloid in solution and away from the catalyst surface. However, the question of the surface activity of both the α-ketoester and the modifier/α-ketoester complex (model b) under reaction conditions remains to be explored. This and the role of oxygen in kink reconstruction are currently the subjects of further investigation.

Conclusion

The enantioselective reactive chemisorption of various sugar molecules on kinked single-crystal platinum surfaces is a manifestation of the intrinsic chirality of the metal kink sites. Systematic changes in the structure of the kink site and also the stereogenic centers on the chemisorbing molecule may be used to deduce important information concerning the adsorption geometry of the metal surface-molecule complex. In addition, a number of fundamental aspects of the cinchona catalyzed enantioselective hydrogenation of α-ketoesters over supported platinum may be investigated by the use of well-defined single-crystal electrodes and the protocols of electrochemical surface science developed over the last 20 years. For example, it appears that the stability of the cinchona chiral auxiliaries is limited on the platinum surface in the presence of 1 atm of hydrogen (although *complete* desorption of the chiral adsorbate could not be achieved via exposure to hydrogen). Also, a random surface distribution of alkaloid on platinum is deduced based on both the indiscriminate uptake of the chiral auxiliaries on various single-crystal platinum surfaces (lack of structural sensitivity) and the finding that, for dihydrocinchonine, free platinum sites are still available for adsorption even for a saturated alkaloid adlayer (imperfect packing of the chemisorbate). More intensive studies of this nature are required before a new model of the action of the cinchona alkaloid in promoting enantioselectivity may be proposed. Our assertion that the supported catalyst particle should be considered as a racemate of *R* and *S* kink sites (whereby preferential adsorption of the alkaloid at a particular chiral site may lead to an enantioselective hydrogenation) needs to be reassessed in the light of the apparent lack of sensitivity to both the adsorption and hydrogen-induced desorption rate of the alkaloid on chiral single-crystal surfaces. Nonetheless, only certain (stable) classes of kink site have so far been considered. It may be that reconstruction of other less stable kink sites is the key to explaining the mechanism of the Orito reaction in terms of a surface excess of *R* or *S* kink sites. The coadsorption of α-ketoesters, hydrogen, and cinchona alkaloid also needs to be explored in this context.

Acknowledgment. G.A.A. gratefully acknowledges the support of the EPSRC (Grant No. M65724), ongoing collaborations on surface chirality with Prof. Juan Feliu, Dr. Enrique Herrero and Dr. Antonio Rodes of the University of Alicante, fruitful discussions concerning the Orito reaction with Prof. Peter Wells at Cardiff University, and Dr. D. Willock for generating the computer modeling images of D- and L-glucose at chiral kinked surfaces. Catherine Harris, David Watson, and Omar Hazzazi are also acknowledged for their help in the preparation of the manuscript.

References and Notes

(1) Orito, Y.; Imai, S.; Nina, S. *J. Chem. Soc. Jpn.* **1979**, *8*, 1118.
(2) Clavilier, J.; Faure, R.; Guinet, G.; Durand, R. *J. Electroanal. Chem.* **1980**, *107*, 205.
(3) Izumi, I. *Adv. Catal.* **1983**, *32*, 215.
(4) Blaser, H.-U. *Tetrahedron Asymm.* **1991**, *2*, 843.
(5) Blaser, H.-U.; Müller, M. In *Heterogeneous Catalysis and Fine Chemicals II*; Guisnet, M., et al., Eds.; Elservier: Amsterdam, The Netherlands, 1991; p 73.
(6) Webb, G.; Wells, P. B. *Catal. Today* **1992**, *12*, 319.
(7) Baiker, A. *J. Mol. Catal.* **1997**, *115*, 473.
(8) Blaser, H.-U.; Jalett, H. P.; Müller, M.; Studer, M. *Catal. Today* **1997**, *37*, 441.
(9) Wells, P. B.; Wilkinson, A. G. *Topics Catal.* **1998**, *5*, 39.
(10) Chang, A. O.; Sharpless, K. B. *J. Org. Chem.* **1997**, *42*, 1587.
(11) Zhang, W.; Loebach, J. L.; Wilson, S. R.; Jacobsen, E. N. *J. Am. Chem. Soc.* **1990**, *112*, 2801.
(12) Parson, R.; Vandernoot, T. *J. Electroanal. Chem.* **1998**, *257*, 9.
(13) Adzic, R. In *Modern aspects of electrochemistry*; White, R. E., Bockris, J. O. M., Conway, B. E, Eds.; Plenum: New York, 1990; p 163.

(14) Petro, J.; Mallat, T.; Polyanszky, E. In *Hydrogen Effects in Catalysis—Fundamental and Practical Applications*; Paal, Z., Menon, P. G., Eds.; Dekker Inc.: New York, 1988.
(15) *Elementary Reaction Steps in Heterogeneous Catalysis*; Joyner, R. W., van Santen, R. A., Eds.; NATO ASI Series C Volume 398; Kluwer: Dordrecht, The Netherlands, 1993.
(16) Mallat, T.; Baiker, A. *Top. Catal.* **1999**, *8*, 115.
(17) For example, see: *Surf. Sci.* **1994**, *299/300*.
(18) Strongin, D. R.; Carrazz, J.; Bare, S. R.; Somorjai, G. A. *J. Catal.* **1987**, *103*, 213.
(19) Hubbard, A. T. *Chem. Rev.* **1988**, *88*, 633.
(20) Yeager, E.; O'Grady, W.; Woo, M. Y. C.; Hagans, P. *J. Electrochem. Soc.* **1978**, *125*, 348.
(21) Ross, P. N. *J. Electroanal. Chem.* **1983**, *76*, 139.
(22) Yamamoto, K.; Kotz, R.; Lehmpfuhl, J.; Kolb, D. M. *J. Electroanal. Chem.* **1979**, *96*, 233.
(23) Hourani, M.; Wieckowski, A. *J. Electroanal. Chem.* **1987**, *227*, 259.
(24) For a recent review of ex situ spectroscopic studies of well-defined electrodes, see also: *Interfacial Electrochemistry − Theory, Experiment and Applications*; Wieckowski, A., Ed.; Dekker: New York, 1999.
(25) Attard, G. A.; Barnes, C. J. *Surfaces*; Oxford University Press, Oxford, U.K., 1998.
(26) Hubbard, A. T.; Stickney, J. L; Rosasco, S. D.; Soriaya, M. P.; Song, D. *J. Electroanal. Chem.* **1983**, *150*, 165.
(27) *Comprehensive Treatise of Electrochemistry*; Bockris, J. O. M., Conway, B. E., Yeager, E., Eds.; Plenum: New York, 1980.
(28) Magnussen, O. M.; Hagebeck, J.; Hotlos, J.; Behm, R. J. *Faraday Discuss*. **1992**, *94*, 329.
(29) Wan, L.-J; Yau, S.-L; Itaya, K. *J. Phys. Chem.* **1995**, 999507.
(30) Wan, L.-J.; Hara, M.; Inukai, J.; Itaya, K. *J. Phys. Chem. B* **1999**, *103*, 6978.
(31) Wan, L.-J.; Suzuki, T.; Sashikata, K.; Okada, J.; Inukai, J.; Itaya, K. *J. Electroanal. Chem*. **2000**, *489*, 189.
(32) Motto, S.; Furuya, N. *J. Electroanal. Chem.* **1984**, *172*, 339.
(33) Chrzanowski, W.; Wieckowski, A. *Langmuir* **1997**, *13*, 5974.
(34) Sun, S. G.; Clavilier, J. *J. Electroanal. Chem.* **1987**, *236*, 95.
(35) Markovic, N. M.; Gasteiger, H. A.; Ross, P. N. *J. Phys. Chem.* **1996**, *100*, 6715.
(36) Morin, S.; Dumont, H.; Conway, B. E. *J. Electroanal. Chem.* **1996**, *412*, 39.
(37) Schmieman, U.; Baltruschat, H. *J. Electroanal. Chem.* **1993**, *347*, 93.
(38) Llorca, M. J.; Feliu, J. M.; Aldaz, A.; Clavilier, *J. Electroanal. Chem.* **1994**, *376*, 151.
(39) Bard, A. J.; Faulkner, L. R. In *Electrochemical Methods, Fundamentals and Applications*; Wiley: New York, 1980.
(40) Ross, P. J. *Chim. Phys*. **1991**, *88*, 1353.
(41) Attard, G. A.; Ahmadi, A. *J. Electroanal. Chem.* **1995**, *389*, 175.
(42) Jablonski, A.; Wandelt, K. *Surf. Sci.* **1991**, *251/252*, 650.
(43) Smith, R. L.; Rohrer, G. S. *J. Solid State Chem.* **1996**, *124*, 104.
(44) McFadden, C. F.; Cremer, P. S.; Gellman, A. J. *Langmuir* **1996**, *12*, 2483.
(45) Van Hove, M. A.; Somorjai, G. A. *Surf. Sci.* **1980**, *92*, 489.
(46) Sholl, D. S. *Langmuir* **1990**, *14*, 862.
(47) Rodes, A.; Llorca, M. J.; Feliu, J. M.; Clavilier, J. *An. Quim. Int. Ed.* **1996**, *92*, 118.
(48) Popovic, K. D.; Tripkovic, A. V.; Adzic, R. R. *J. Electroanal. Chem.* **1992**, *339*, 227.
(49) Kokkinidis, G.; Leger, J. M.; Lamy, C. *J. Electroanal. Chem*. **1988**, *242*, 221.
(50) Morrison, R. T.; Boyd, R. N. *Organic Chemistry*, 3rd ed.; Allyn and Bacon: Boston, MA, 1973.
(51) Attard, G. A.; Clavilier, J.; Feliu, J. M. In *Physical Chemistry of Chirality*; Hicks, J., Ed.; ACS Symposium Series, in press.
(52) Attard, G. A.; Ahmadi, A.; Feliu, J. M.; Rodes, A.; Herrero, E.; Blais, S.; Jerkiewicz, G. *J. Phys. Chem. B* **1999**, *103*, 1381.
(53) Harris, C. A.; Attard, G. A. Manuscript in preparation.
(54) Harris, C. A.; Attard, G. A.; Herrero, E.; Feliu, J. M. Manuscript in preparation.
(55) Power, T. D.; Sholl, D. S. *Topics in Catalysis* accepted for publication.
(56) Gellman, A. J.; Horvath, J. D.; Buelow, M. T. *J. Mol. Catal. A* submitted for publication.
(57) Margitfalvi, J. L.; Hegedus, M.; Tfirst, E. *Tetrahedron Asymm.* **1996**, *7*, 571.
(58) Margitfalvi, J. L.; Hegedus, M. *J. Mol. Catal. A* **1996**, *107*, 281.
(59) Margitfalvi, J. L.; Hegedus, M.; Tfirst, E. *Stud. Surf. Sci. Catal.* **1996**, *101*, 241.
(60) Margitfalvi, J. L.; Tfirst, E. *J. Mol. Catal.* A **1999**, *139*, 81.
(61) Raval, R.; Baddeley, C. J.; Muryn, C.; Lorenzo, M. O. *Nature* **2000**, *404*, 376−379.
(62) Carley, A. F.; Rajumon, M. K.; Roberts, M. W.; Wells, P. B. *J. Chem. Soc., Faraday Trans.* **1995**, *91*, 2167.
(63) Castonguay, M.; Roy, J.-R.; Rochefort, A.; McBreen, P. H. *J. Am. Chem. Soc.* **2000**, *122*, 518.
(64) Burgi, T.; Atamny, F.; Schlogl, R.; Baiker, A. *J. Phys. Chem. B* **2000**, *104*, 5953.
(65) Wynberg, H. *Topics in Stereochemistry*; Wiley: New York 1986; Vol. 16, p 87.
(66) Hazzazi, O.; Attard, G. A. To be published.
(67) Bond, G.; Wells, P. B. *J. Catal.* **1994**, *150*, 329.
(68) Evans, T.; Woodhead, A. P.; Gutierrez-Sosa, A.; Thornton, G.; Hall, T. J.; Davis, A. A.; Young, N. A.; Wells, P. B.; Oldman, R. J.; Plaskkevych, O.; Vahtras, O.; Agren, H.; Carravetta, V. *Surf. Sci.* **2000**, *436*, 4691.
(69) Wells, P. B.; Simons, K. E.; Slipszenko, J. A.; Griffiths, S. P.; Ewing, D. F. *J. Mol. Catal. A* **1999**, *146*, 159.